ACS OMEGA

Open Access

http://pubs.acs.org/journal/acsodf

Article

Thioflavin-T: A Quantum Yield-Based Molecular Viscometer for Glycerol−Monohydroxy Alcohol Mixtures

Puspal Mukherjee* and Sintu Ganai*

Cite This: *ACS Omega* 2023, 8, 36604−36613

Read Online

ACCESS | Metrics & More | Article Recommendations | Supporting Information

ABSTRACT: Molecular rotor dye thioflavin T (ThT) is almost non-fluorescent in low-viscosity solvents but highly fluorescent when bound to amyloid fibrils. This unique property arises from the rotation of the dimethylaniline moiety relative to the benzothiazole moiety in the excited state, which drives the dye from an emissive locally excited state to a twisted intramolecular charge-transfer state. This process is viscosity-controlled, and therefore, we can use the quantum yield of ThT to assess the viscosity of the environment. In this study, we have investigated the quantum yield of ThT (φ_{ThT}) in various compositions of six alcoholic solvent mixtures of glycerol with methanol, ethanol, *n*-propanol, *iso*-propanol, *n*-butanol, and *tert*-butanol. We have proposed an empirical model using φ_{ThT} as a function of the mole fraction of glycerol to estimate the interaction parameters between the components of the solvent mixtures. This analysis allowed us to predict the extent of nonideality of the solvent mixtures. The Förster−Hoffmann- and Loutfy−Arnold-type power law relationship was established between the quantum yield of ThT and bulk viscosity for solvent mixtures of methanol, ethanol, *n*-butanol, and *tert*-butanol with glycerol, and it was found to be similar in nature in all the four mixtures. Applying this knowledge, we proposed a methodology to quantify and predict the bulk viscosity coefficient values of several compositions of *n*-propanol−glycerol and *iso*-propanol−glycerol mixtures which have not been previously documented.

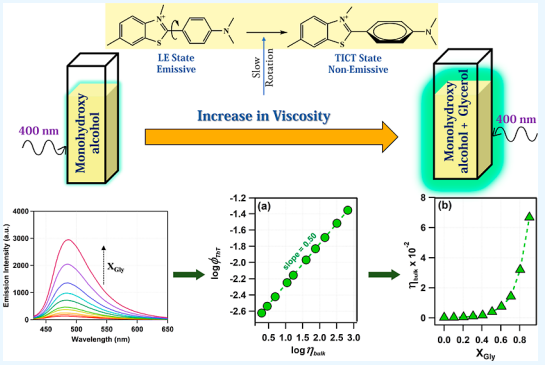

1. INTRODUCTION

Thioflavin-T (ThT, Scheme 1) is a well-established marker for β-amyloid fibrils which are associated in a wide range of protein disorder diseases like Alzheimer's, Parkinson's, and prion diseases.[1−4] Thioflavin-T exhibits weak fluorescence emission in water, but upon binding with amyloid fibrils, it undergoes a remarkable enhancement in emission intensity.[1−4] ThT selectively binds to DNA, RNA, and enzymes, and the same type of drastic fluorescence increase has been observed in the ThT−biomolecule complex.[5−9] Such an increase in emission intensity is not only unique to ThT. It belongs to a class of dyes known as molecular rotors.[1,10−13] Molecular rotor dyes experience internal rotation in the excited state, which controls their emissive properties.[1,10−13] In the ground state, the dihedral angle between the benzothiazole and dimethylaniline moiety around the C−C bond of ThT is approximately 37°.[1,14−16] The relative orientation of those two moieties around the C−C bond changes in the excited state.[1,14−18] Upon excitation, ThT molecules populate a locally excited (LE) state which has a similar geometry like ground state, and the fluorescence emission of ThT primarily originates from this state.[1,14−18] Subsequently, ThT undergoes a twisting motion of the dimethylaniline moiety with respect to the benzothiazole fragment, resulting an angle of ∼90°.[1,14−18] Significant charge redistribution within the molecular framework accompanies this motion, and therefore, this process is known as twisted intramolecular charge transfer (TICT).[1,14−20] The TICT state is a dark nonemissive state of ThT.[1,14−20] The LE to TICT conversion is generally considered to be barrierless and ultrafast in nature, and any external factor that hinders this channel leads to an increase in the fluorescence intensity of ThT.[1,17,18,21−23]

Scheme 1. Chemical Structure of Thioflavin-T

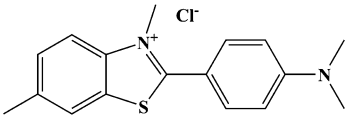

Binding with amyloid fibrils and other biomolecules prevents the internal rotation of ThT and, thus, increases the fluorescence intensity. Macromolecular hosts can also impose spatial restrictions, and a similar phenomenon has been observed when ThT interacts with micelles, cellulose nanocrystals, and

Received: August 28, 2023
Accepted: September 6, 2023
Published: September 18, 2023

cyclodextrin or cucurbit[n]uril compounds.[24−27] The viscosity of the medium becomes the governing factor for ThT emission in liquid media, as the molecular rotation is significantly controlled by the presence of viscous drag.[1,24,28,29] Several studies have explored the effect of viscosity on the excited-state dynamics of the molecular rotors, and they have been used as viable viscosity sensors in biological systems.[30−33] Singh et al. have studied the excited-state dynamics of ThT using ultrafast spectroscopy in aqueous solutions, amyloid fibrils, in an acetonitrile−ethylene glycol mixture and inside the AOT reverse micelle.[28,34−36] Amdursky et al. have studied the temperature dependence of fluorescence properties of ThT in glass forming liquids.[37] The enhancement of ThT fluorescence intensity with viscosity has been very prominently shown in deep eutectic solvents by Gautam et al. and in ionic liquids by Singh et al.[38,39] Stsiapura et al. have shown that in low-viscosity solvents like water and ethanol, the charge-transfer process influences the dynamics of TICT formation.[40] A temperature-dependent study of ThT and auramine O in *n*-propanol, *n*-butanol, and *n*-pentanol has found direct correlation between viscosity and steady-state fluorescence properties.[41] Such studies along with many others have illustrated the influence of viscosity of the medium on the rate of LE → TICT transition and the barrierless characteristics of the excited-state potential energy surface. Since LE → TICT transition involves significant charge transfer, solvent polarity influences this process.[37,40−42] For example, Stsiapura et al. have recorded transient absorption spectroscopic data for ThT in 12 different solvents at room temperature and explored static and dynamic solvation effects on the charge-transfer rate based on Marcus theory.[42] Solvation dynamics can control the process, but the overall excited-state lifetime of ThT is shorter than the solvent relaxation time in most of the solvents.[37,40−42] There are other reports that suggest the existence of multiple TICT states along with conical intersections in the potential energy surface (PES) of the first singlet excited state. Specifically, Mukherjee et al. have demonstrated that a second TICT state can be formed via rotation of the dimethylamine moiety of ThT, and this process contributes to the excited-state dynamics significantly in chlorinated solvents like chloroform and dichloromethane.[43] Ghosh and Palit have suggested the involvement of triplet state of ThT in the excited-state dynamics.[44] All the studies agree to the fact that all the TICT states are nonemissive, whereas the LE state is the only emissive state of ThT.

The preceding discussion highlights that the photophysical properties of ThT can be used to quantify the viscosity of the surrounding medium. Commonly, bulk viscosities are measured by capillary-based methods. While Ostwald's viscometer is generally used for teaching purposes, Cannon-Ubbelohde-type capillary viscometers are used for accurate viscosity values.[45,46] Rolling ball-type viscometers are also used for the measurement of liquid viscosities.[47] Apart from these common experimental methods, the bulk viscosity of pure liquids has been measured using acoustics spectroscopy.[48,49] Molecular rotors have also been used to sense viscosity changes in various biomolecular environments.[50,51] Molecular rotors do not actually encounter bulk viscosity. Instead, the viscous drag imposed on the fragmental rotation is by the solvation shell around the molecule.[34−44] This is known as microviscosity, and molecular rotor dyes sense the microviscosity around them. The composition and properties of the solvation shell can be different from the bulk composition, especially in solvent mixtures, in confined environments, or in a system having dynamic heterogeneity.[34−44] Therefore, quantification of the environmental viscosity by observing photophysical quantities is not straightforward. There are some examples of estimation of viscosity in cells and other biological systems.[30−33] However, these types of studies have been mostly carried out in confined spaces and sometimes involve designing complicated molecules.[30−33] We wanted to explore whether a common photophysical property like fluorescence quantum yield can be quantitatively related/calibrated to bulk viscosity in the liquid phase and be used to estimate the unknown viscosity of a binary solvent system. ThT is a perfect candidate for that purpose because its photophysics is well established; it only shows emission from the LE state, and therefore, its emission spectrum is free from contribution of radiative transitions from other TICT states. The easiest way to vary viscosity is either to study a large range of solvents or to use solvent mixtures where one component has a high viscosity. However, the nonpolar and chlorinated solvents were to be avoided due to the unusual photophysical responses of ThT in them. We therefore decided to undertake a study on binary mixtures of glycerol and monohydric alcohols, namely, methanol, ethanol, *n*-propanol, *iso*-propanol, *n*-butanol, and *tert*-butanol. As both components of the binary mixtures are alcohols, any sudden changes in the bulk properties are not expected. Since glycerol has very high viscosity compared to the others, the variations of viscosity in these mixtures are enormous. In the following sections of this report, we outline a methodology for predicting the unknown bulk viscosity of *n*-propanol−glycerol and *iso*-propanol−glycerol mixtures by simple measurement and analysis of ThT quantum yield along with the determination of the solvent interaction parameter of the constituents of the binary solvent mixtures.

2. EXPERIMENTAL SECTION

2.1. Materials. HPLC-grade methanol, *n*-propanol, *iso*-propanol, *n*-butanol, and *tert*-butanol were purchased from Spectrochem, India. Ethanol was purchased from Himedia, and molecular biology-grade glycerol was purchased from Merck, India. All the solvents apart from glycerol were distilled prior to use. Thioflavin-T (ThT) was purchased from SRL, India, and recrystallized twice from ethanol. The concentration of ThT was kept below 10 μM in all of the experiments to avoid any aggregation-induced effect.

2.2. Methods. The UV−visible spectra were recorded in a Shimadzu UV-1900 commercial spectrophotometer, and the fluorescence spectra were recorded in an Agilent Cary Eclipse spectrofluorimeter. All of the measurements were performed in quartz cuvettes of 1 cm path length. ThT solutions were prepared by thoroughly dissolving recrystallized ThT in pure solvents, followed by filtration to remove any undissolved particles. ThT dissolved in *n*-butanol was used as the reference in quantum yield measurements.[14,42] All the steady-state absorption and emission spectra of ThT in pure solvent and solvent mixtures were recorded under the same experimental conditions. Fluorescence quantum yields were calculated using eq 1.

$$\varphi_{\mathrm{ThT}} = \varphi_{\mathrm{ref}} \times \frac{I_{\mathrm{ThT}}}{I_{\mathrm{ref}}} \times \frac{A_{\mathrm{ref}}^{\lambda_{\mathrm{ex}}}}{A_{\mathrm{ThT}}^{\lambda_{\mathrm{ex}}}} \times \frac{n_i^2}{n_{\mathrm{ref}}^2} \quad (1)$$

In eq 1, φ_{ThT} and φ_{ref} are the quantum yields of ThT in a particular medium and ThT in *n*-butanol, respectively. I_{ThT} and I_{ref} are the integrated area of emission for $A_{\mathrm{ThT}}^{\lambda}{}_{\mathrm{ex}}$ and $A_{\mathrm{ref}}^{\lambda}{}_{\mathrm{ex}}$ are the absorbance indexes at the excitation wavelength of ThT in a

https://doi.org/10.1021/acsomega.3c06428
ACS Omega 2023, 8, 36604−36613

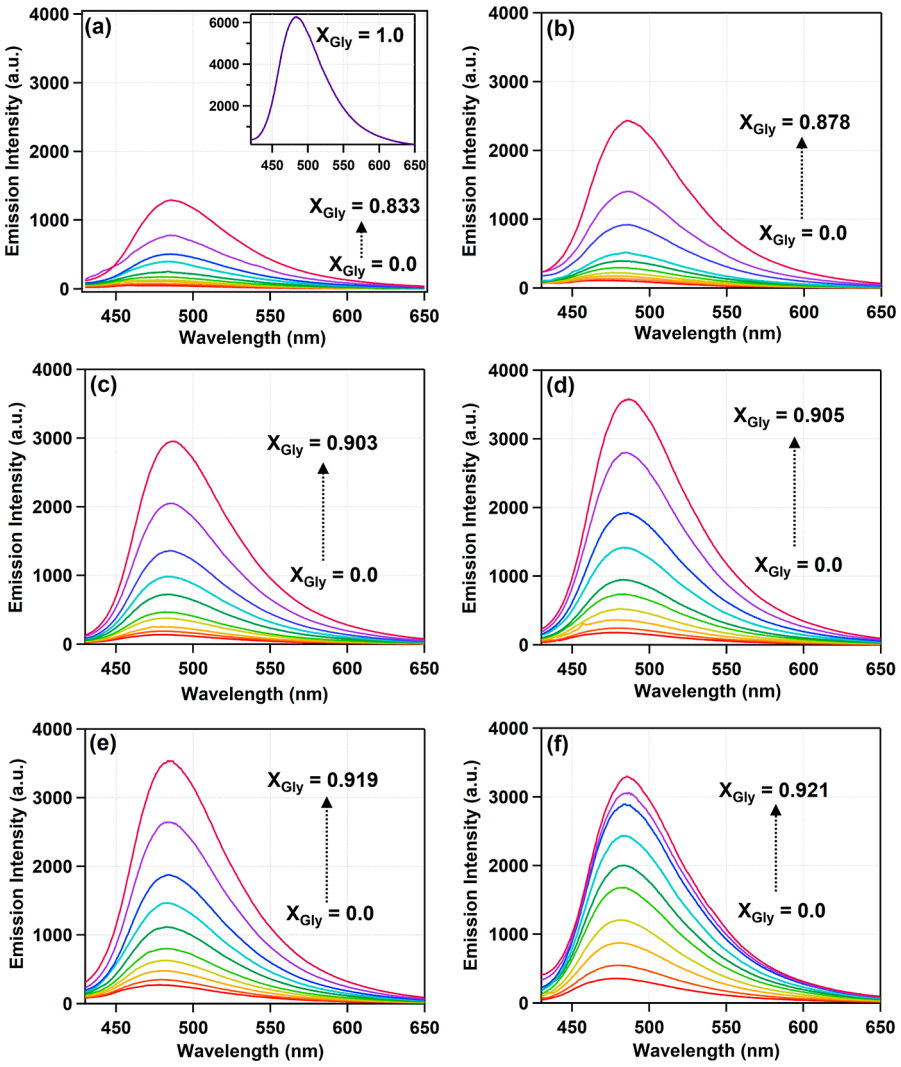

Figure 1. Emission spectra of thioflavin T in different compositions of the solvent mixtures: (a) methanol−glycerol, (b) ethanol−glycerol, (c) *n*-propanol−glycerol, (d) *iso*-propanol−glycerol, (e) *n*-butanol−glycerol, and (f) *tert*-butanol−glycerol. X_{Gly} indicated the mole fraction of glycerol. The spectra of ThT in pure glycerol are shown in the inset of (a). The excitation wavelength in all of the cases is 400 nm.

medium and *n*-butanol, respectively. n_i and n_{ref} are the refractive indexes of the solvent and *n*-butanol. φ_{ref} was taken from refs 14 and 42. In order to prevent any artifacts caused by variations in excitation wavelengths, the same excitation light of 400 nm was used in all cases. The background Raman scattering from the solvent medium was removed from the emission spectra of ThT for the quantum yield calculations. To estimate the error in the quantum yield value measurements, we have repeated the experiments in a few randomly selected compositions for each of the solvent mixtures and found the maximum error in quantum yield estimation to be ±2%. Refractive index measurements of the *n*-propanol−glycerol mixture and *iso*-propanol−glycerol mixture were performed on a commercial Abbe refractometer (Atago, Japan). For reference, we used the refractive index value of pure water at room temperature. Experiments involving *tert*-butanol were performed keeping the room temperature at 30 °C since *tert*-butanol can freeze at lower temperatures. All other experiments were performed at 25 °C.

3. RESULTS AND DISCUSSION

Considering the deliberations presented in the Introduction Section, it is reasonable to infer that the emission spectra of ThT in alcoholic solvents are primarily the radiative decay of population from the LE state of the molecule which can help us correlate the emissive property with a bulk solvent property. We, therefore, measured the absorption and emission spectra of ThT in the various compositions of the solvent mixtures, namely, methanol−glycerol, ethanol−glycerol, *n*-propanol−glycerol, *iso*-propanol−glycerol, *n*-butanol−glycerol, and *tert*-butanol−glycerol. The representative absorption spectra are shown in Supporting Information Figure S1. The fluorescence emission spectra of ThT in various compositions of the solvent mixtures mentioned are presented in Figure 1. In each case, we recorded the spectra in nine different compositions along with the pure solvents. The intensity of the emission spectra of ThT is inherently controlled by the viscosity of the solvent medium as highlighted in the Introduction Section. Glycerol has a viscosity of 950 cP at room temperature, which is tremendously high compared to the viscosity of methanol (0.6 cP), ethanol (1.105 cP), *n*-propanol (1.97 cP), *iso*-propanol (2.098 cP), *n*-butanol (2.568 cP), and *tert*-butanol (3.155 cP).[52−54] Therefore, the viscosity of the solvent mixtures studied varied over a wide range, and the change in the intensity of the emission spectra of ThT in these mixtures is distinctly noticeable, as depicted in

https://doi.org/10.1021/acsomega.3c06428
ACS Omega 2023, 8, 36604−36613

Table 1. Absorption Maxima, Emission Maxima, Stokes Shift Values, and Quantum Yield of Thioflavin-T in Six Glycerol−Monohydroxy Alcohol Solvent Mixtures along with the Known Values of Bulk Viscosity of the Mixtures

X_1	X_2	absorption maxima in cm^{-1} (in nm)	emission maxima in cm^{-1} (in nm)	Stokes shift in cm^{-1}	quantum yield of ThT[a]	viscosity (cP)[b,c]
			Glycerol (1) + Methanol (2)			
0.000	1.000	24073.18 (415.4)	21186.44 (472.0)	2886.74	0.0005	0.6
0.058	0.942	24026.91 (416.2)	21164.02 (472.5)	2862.89	0.0012	1.8
0.122	0.878	23969.32 (417.2)	21097.05 (474.0)	2872.27	0.0018	4.8
0.192	0.808	23934.9 (417.8)	21008.40 (476.0)	2926.50	0.0022	7.7
0.270	0.730	23877.75 (418.8)	20898.64 (478.5)	2979.10	0.0030	13
0.357	0.643	23843.59 (419.4)	20768.43 (481.5)	3075.15	0.0041	28
0.454	0.546	23809.52 (420.0)	20682.52 (483.5)	3127.0	0.0063	58
0.564	0.436	23775.56 (420.6)	20597.32 (485.5)	3178.24	0.0082	130
0.689	0.311	23741.69 (421.2)	20554.98 (486.5)	3186.71	0.0128	250
0.833	0.167	23707.92 (421.8)	20533.88 (487.0)	3174.04	0.0200	630
1.000	0.000	23707.92 (421.8)	20576.13 (486.0)	3131.79	0.0963	950
			Glycerol (1) + Ethanol (2)			
0.000	1.000	23900.57 (418.4)	21276.6 (470.0)	2623.98	0.0013	1.23
0.082	0.918	23866.35 (419.0)	21164.02 (472.5)	2702.33	0.0021	2.81
0.167	0.833	23820.87 (419.8)	21008.4 (476.0)	2812.46	0.0026	6.28
0.255	0.745	23820.87 (419.8)	20876.83 (479.0)	2944.04	0.0034	13.70
0.348	0.652	23798.19 (420.2)	20811.65 (480.5)	2986.54	0.0048	29.01
0.444	0.556	23775.56 (420.6)	20746.89 (482.0)	3028.67	0.0063	59.24
0.545	0.455	23764.26 (420.8)	20639.83 (484.5)	3124.42	0.0089	115.76
0.651	0.349	23741.69 (421.2)	20597.32 (485.5)	3144.37	0.0129	214.68
0.762	0.238	23730.42 (421.4)	20576.13 (486.0)	3154.29	0.0221	374.08
0.878	0.122	23696.68 (422.0)	20576.13 (486.0)	3120.55	0.0373	605.47
1.000	0.000	23707.92 (421.8)	20576.13 (486.0)	3131.79	0.0963	950.0
			Glycerol (1) + *n*-Propanol (2)			
0.000	1.000	23900.57 (418.4)	20898.64 (478.5)	3001.93	0.0024	
0.103	0.897	23866.35 (419.0)	20811.65 (480.5)	3054.69	0.0029	
0.205	0.795	23832.22 (419.6)	20790.02 (481.0)	3042.20	0.0038	
0.306	0.694	23809.52 (420.0)	20746.89 (482.0)	3062.64	0.0057	
0.407	0.593	23798.19 (420.2)	20725.39 (482.5)	3072.80	0.0070	
0.507	0.493	23764.26 (420.8)	20661.16 (484.0)	3103.10	0.0108	
0.607	0.393	23730.42 (421.4)	20639.83 (484.5)	3090.59	0.0148	
0.706	0.294	23707.92 (421.8)	20618.56 (485.0)	3089.36	0.0203	
0.805	0.195	23696.68 (422.0)	20597.32 (485.5)	3099.36	0.0304	
0.903	0.097	23674.24 (422.4)	20554.98 (486.5)	3119.26	0.0440	
1.000	0.000	23707.92 (421.8)	20576.13 (486.0)	3131.79	0.0963	
			Glycerol (1) + *iso*-Propanol (2)			
0.000	1.000	23957.83 (417.4)	20898.64 (478.5)	3059.19	0.0027	
0.105	0.895	23889.15 (418.6)	20833.33 (480.0)	3055.82	0.0038	
0.208	0.792	23866.35 (419.0)	20833.33 (480.0)	3033.02	0.0050	
0.311	0.689	23832.22 (419.6)	20790.02 (481.0)	3042.20	0.0073	
0.413	0.587	23798.19 (420.2)	20725.39 (482.5)	3072.80	0.0106	
0.513	0.487	23764.26 (420.8)	20703.93 (483.0)	3060.32	0.0138	
0.612	0.388	23752.97 (421.0)	20682.52 (483.5)	3070.45	0.0209	
0.711	0.289	23719.17 (421.6)	20618.56 (485.0)	3100.61	0.0286	
0.808	0.192	23696.68 (422.0)	20597.32 (485.5)	3099.36	0.0415	
0.905	0.095	23685.46 (422.2)	20554.98 (486.5)	3130.47	0.0540	
1.000	0.000	23696.68 (422.0)	20576.13 (486.0)	3120.55	0.0963	
			Glycerol (1) + *n*-Butanol (2)			
0.000	1.000	23889.15 (418.6)	20876.83 (479.0)	3012.33	0.0043	2.57
0.122	0.878	23854.96 (419.2)	20855.06 (479.5)	2999.90	0.0058	4.78
0.239	0.761	23820.87 (419.8)	20790.02 (481.0)	3030.85	0.0081	8.90
0.350	0.650	23786.87 (420.4)	20746.89 (482.0)	3039.98	0.0110	16.52
0.455	0.545	23775.56 (420.6)	20703.93 (483.0)	3071.62	0.0141	30.56
0.556	0.444	23741.69 (421.2)	20682.52 (483.5)	3059.17	0.0197	56.24
0.653	0.347	23719.17 (421.6)	20682.52 (483.5)	3036.64	0.0260	102.83
0.745	0.255	23707.92 (421.8)	20661.16 (484.0)	3046.76	0.0334	186.66
0.834	0.166	23696.68 (422.0)	20639.83 (484.5)	3056.85	0.0471	336.12
0.919	0.081	23696.68 (422.0)	20618.56 (485.0)	3078.13	0.0637	600.13
1.000	0.000	23696.68 (422.0)	20576.13 (486.0)	3120.55	0.0963	950.0

https://doi.org/10.1021/acsomega.3c06428
ACS Omega 2023, 8, 36604−36613

Table 1. continued

X_1	X_2	absorption maxima in cm^{-1} (in nm)	emission maxima in cm^{-1} (in nm)	Stokes shift in cm^{-1}	quantum yield of ThT[a]	viscosity (cP)[b,c]
			Glycerol (1) + *tert*-Butanol (2)			
0.000	1.000	23889.15 (418.6)	20920.5 (478.0)	2968.65	0.0050	3.15
0.126	0.874	23866.35 (419.0)	20855.06 (479.5)	3011.29	0.0077	8.22
0.246	0.754	23854.96 (419.2)	20811.65 (480.5)	3043.31	0.0122	18.72
0.358	0.642	23820.87 (419.8)	20768.43 (481.5)	3052.44	0.0171	37.85
0.465	0.535	23798.19 (420.2)	20725.39 (482.5)	3072.80	0.0240	69.04
0.566	0.434	23741.69 (421.2)	20703.93 (483.0)	3037.76	0.0292	115.12
0.661	0.339	23741.69 (421.2)	20682.52 (483.5)	3059.17	0.0358	177.45
0.752	0.248	23707.92 (421.8)	20639.83 (484.5)	3068.08	0.0429	255.31
0.839	0.161	23685.46 (422.2)	20597.32 (485.5)	3088.13	0.0479	345.77
0.921	0.079	23674.24 (422.4)	20597.32 (485.5)	3076.92	0.0520	444.00
1.000	0.000	23696.68 (422.0)	20576.13 (486.0)	3120.55	0.0780	544.03

[a]The maximum error associated with the measurements ±2%. [b]Viscosity data are taken from refs 56−60. [c]The viscosity values of glycerol−*n*-propanol and glycerol−*iso*-propanol mixtures are not reported in the literature and estimated using our proposed methodology in the next section.

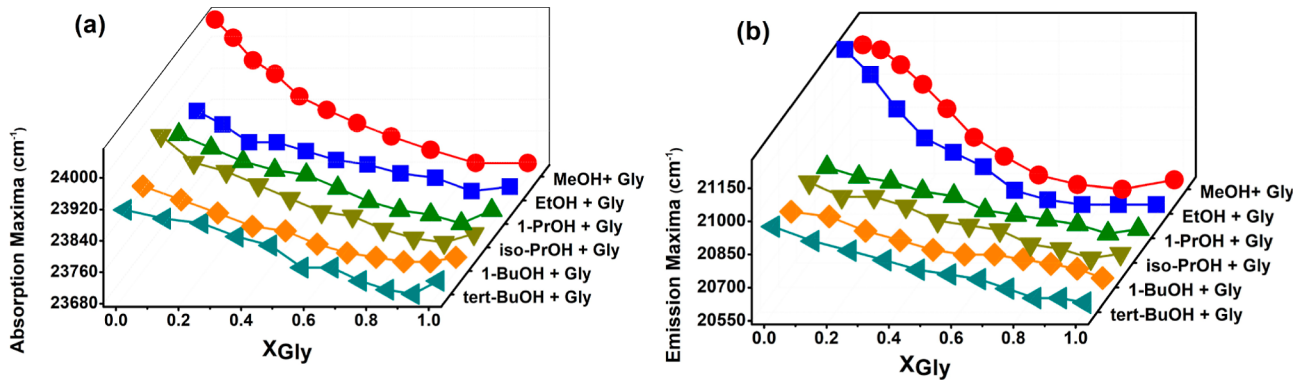

Figure 2. (a) Absorption and (b) emission maxima of thioflavin T as a function of the mole fraction of glycerol in different glycerol−monohydroxy alcohol solvent mixtures. Gly indicates glycerol.

Figure 1. We would like to point out here that the gradual increase in the intensity of emission spectra with increasing glycerol mole fraction in the mixture was observed in all the cases, and no sudden unique feature appeared. In Figure 1, the emission spectra of ThT in glycerol are shown in the inset since the intensity is very high compared to others. The steady-state absorption and emission spectra recorded in pure solvents was found to match with previous reports.[15,40,43]

The emission spectra shown in Figure 1 are not corrected for their absorbance at excitation wavelength, and therefore, their intensity should not be directly compared. Moreover, we are reiterating that the *tert*-butanol−glycerol mixture was studied at 30 °C instead of 25 °C unlike the other solvent mixtures. Nonetheless, Figure 1 shows the trend in the increase of fluorescence intensity and, in turn, medium viscosity.

Before further exploration, it is necessary to discuss the shift in the spectra. The excited-state deactivation process of ThT involves the formation of the TICT state from the LE state, which is viscosity-controlled.[1,14,15,18,40] However, the excitation from the ground to the excited state and the subsequent deactivation process of the molecules are also influenced by the polarity of the medium.[40−42] The dielectric constant of the solvents studied ranged from 10.9 (*tert*-butanol) to 46.5 (glycerol).[55] To examine the effect of this variation, the spectral shifts of ThT were recorded. Table 1 presents the observed absorption, emission maxima, and Stokes shift of ThT in various compositions of glycerol−alcohol solvent mixtures. Figure 2 represents the variation of these maxima as a function of the mole fraction of the glycerol content in those mixtures. In each of the solvent mixtures, with increase in glycerol content, the absorption and emission maxima of ThT showed a bathochromic shift. From Figure 2a, we can see that the largest range of shift in absorption maxima with increase in glycerol content in the mixture was found in a methanol−glycerol mixture, whereas a largest range of shift for emission maxima was observed in the ethanol−glycerol mixture (Figure 2b). The Stokes shift values are also similar and varied within ∼2800 to ∼3200 cm^{-1}. These small changes in spectral parameters showed that the extent of influence of polarity on the excited-state properties of ThT is small or similar in the solvent mixtures studied here. So, we can safely assume that viscosity is the major and primary factor of changes in emission spectra.

We measured the quantum yield (φ_{ThT}) of ThT using the procedure described in the Experimental Section. To calculate the quantum yield values, we needed a refractive index for each experimental composition of solvent mixtures. The refractive index values of exact compositions of the methanol−glycerol solvent mixture used in this study at 25 °C are reported in the literature.[56] For ethanol−glycerol, *n*-butanol−glycerol, and *tert*-butanol−glycerol mixtures, the refractive index values are reported in several compositions but not at the exact compositions of the mixtures prepared by us.[57−60] To estimate the values at our experimental compositions, we fitted the reported data using a second-order polynomial equation and evaluated the required values from it. The literature values along with the estimated refractive indexes are reported in Supporting Information Table S2. Despite conducting an extensive literature search, we could not find any existing reports on

https://doi.org/10.1021/acsomega.3c06428
ACS Omega 2023, 8, 36604−36613

refractive index values for *n*-propanol−glycerol and *iso*-propanol−glycerol mixtures. Therefore, we measured the refractive index values of those two solvent mixtures at our experimental compositions, which are reported in Supporting Information Table S3. These measured values were used for quantum yield calculation.

The calculated values of φ_{ThT} are listed in Table 1. To validate our measurements, we compared the values in pure solvents with the reported values and found them to be comparable.[1,15,40,41] φ_{ThT} gradually increased with increasing concentration of glycerol in each mixture, which correlates with the increase in fluorescence emission intensity shown in Figure 1. However, the specific variation pattern differs for each case, and φ_{ThT} exhibits a nonlinear relationship with the glycerol concentration across all systems. In Figure 3, we have shown

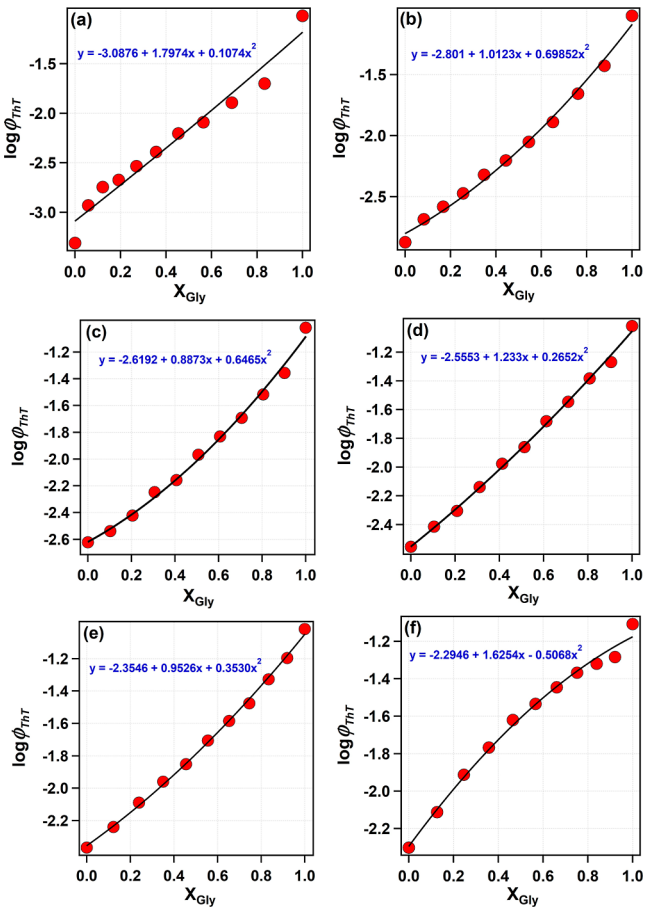

Figure 3. Plot of variation of logφ_{ThT} against the mole fraction of glycerol in (a) methanol−glycerol, (b) ethanol−glycerol, (c) *n*-propanol−glycerol, (d) *iso*-propanol−glycerol, (e) *n*-butanol−glycerol, and (f) *tert*-butanol−glycerol solvent mixtures. X_{Gly} indicated the mole fraction of glycerol. The black lines indicate fitting using eq 4.

the variation of log φ_{ThT} vs mole fraction of glycerol (X_{Gly}) for each system. The trend of log φ_{ThT} also showed a nonlinear dependence on X_{Gly}, indicating the nonideality of the solvent mixtures. The nonideality originates from a specific interaction between the components of the mixture.[56−60] Since φ_{ThT} is a direct manifestation of viscosity of the medium, we followed the Grunberg−Nissan model for liquid mixture viscosity to quantitatively analyze the variation of φ_{ThT}.[61,62] The simplest approach would be to model φ_{ThT} of the solvent mixtures to be a linear combination of the values in pure components, but it only works for ideal cases. Grunberg−Nissan developed an empirical model to estimate the viscosity of solvent mixtures.[61,62] It follows an Arrhenius type of mixing model with the incorporation of a solvent−solvent interaction parameter.[61,62] As per the proposition of the Grunberg−Nissan model, this interaction coefficient depends on temperature but does not change with the composition of the mixture. In the case of viscosity, the interaction coefficient can be directly related to the activity coefficients of the pure components via Raoult's law.[61,62] Thus, it can be used to estimate the deviation of the solvent mixture from ideality. Similarly, we propose that the quantum yield of ThT in any composition of a specific binary solvent mixture can be modeled as follows

$$\log \varphi_{12} = x_1 \log \varphi_1 + x_2 \log \varphi_2 + x_1 x_2 \delta \quad (2)$$

Here, log φ_{12}, log φ_1, and log φ_2 are the quantum yields of ThT in the mixture, in pure component 1, and in pure component 2, respectively; x_1 and x_2 are the mole fractions of components 1 and 2 in the mixture, and δ is the interaction parameter. This interaction parameter δ may depend on temperature but is assumed to not change with the composition of a particular binary solvent mixture. We can rewrite eq 2 by substituting x_2 with 1-x_1 as follows

$$\log \varphi_{12} = -x_1^2 \delta + x_1(\log \varphi_1 - \log \varphi_2 + \delta) + \log \varphi_2 \quad (3)$$

Equation 3 offers the advantage of using only x_1 to fit the data of log φ_{12}. We used eq 3 to fit the data of log φ_{ThT} against X_{Gly}, and the fitting curves along with the fitting equations are also shown in Figure 3. The interaction parameters for each of our experimental systems are reported in Table 2, and these values

Table 2. Interaction Parameter δ in eq 2 and the Slope α in eq 5 for Six Glycerol−Monohydroxy Alcohol Mixtures

solvent mixture	δ	α
glycerol + methanol	−0.1074	0.502
glycerol + ethanol	−0.6985	0.495
glycerol + *n*-propanol	−0.6465	0.49−0.50 (predicted range)
glycerol + *iso*-propanol	−0.2652	0.49−0.50 (predicted range)
glycerol + *n*-butanol	−0.3530	0.491
glycerol + *tert*-butanol	0.5068	0.489

indicate the extent of interaction between the two components of the binary mixture. Generally, to predict deviation from ideally of liquid mixtures, excess thermodynamic quantities are measured.[56−60] Spectroscopic properties such as solvatochromic shift were also used to predict synergistic or preferential interactions.[63] However, estimation of the solvent−solvent interaction using quantum yield data is rare. Since the concentration of ThT is extremely low compared to the solvents, the overall system will be negligibly perturbed. Therefore, the modeling proposed here can represent deviation from ideality. The δ parameters found from this analysis showed that the interaction is highest between ethanol and glycerol, followed by *n*-propanol−glycerol. Interestingly, the only positive δ value was shown by the *tert*-butanol−glycerol mixture, which signifies that the nature of the interaction is opposite in this case. Based on the discussion on the available models of nonideality, it may be concluded that a positive δ value means negative deviation from ideality and a negative δ parameter means positive deviation from ideality.[61,62] Accordingly, we can say that the binary mixtures of glycerol with methanol, ethanol, *n*-

https://doi.org/10.1021/acsomega.3c06428
ACS Omega 2023, 8, 36604−36613

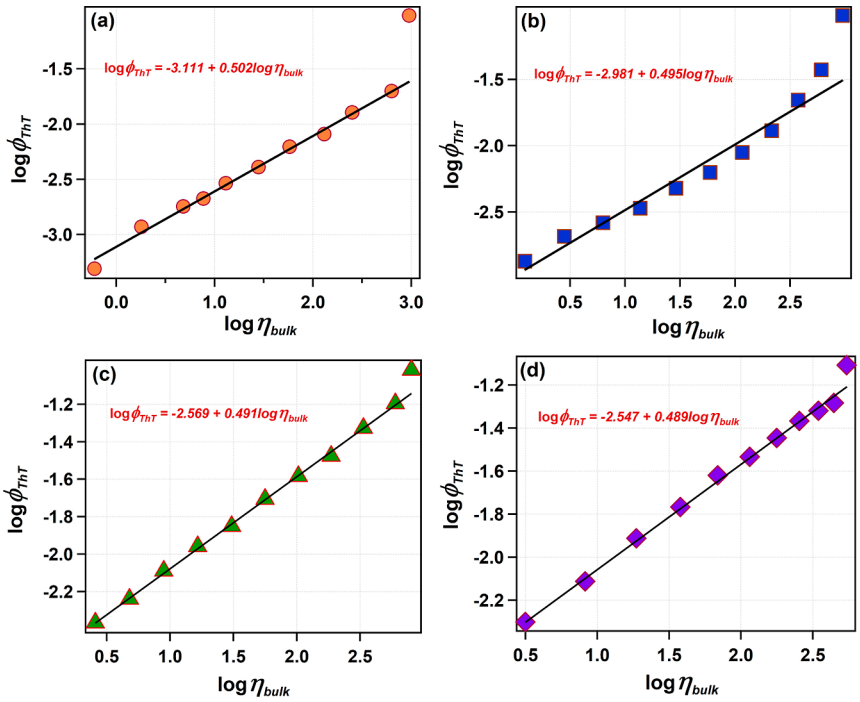

Figure 4. Plot of variation of log φ_{ThT} against log η_{bulk} for (a) methanol−glycerol, (b) ethanol−glycerol, (c) *n*-butanol−glycerol, and (d) *tert*-butanol−glycerol solvent mixtures. The black lines indicate linear fitting excluding the point for pure glycerol.

propanol, *iso*-propanol, and *n*-butanol showed positive deviation from ideality, whereas a mixture of glycerol with *tert*-butanol showed negative deviation from ideality. To check whether these mixtures actually deviate from ideality and their nature of interaction, we have used the measured refractive index values of the *n*-propanol−glycerol and *iso*-propanol−glycerol mixtures and calculated the excess molar refractivity values as per the method given in Supporting Information Scheme S1. We found that both the mixtures showed positive deviation from ideality as predicted by our model. The maximum deviation from ideality occurs for composition with a mole fraction around 0.5 in each case (Supporting Information Figure S2). We cannot, however, compare the interaction parameters obtained from our analysis to the excess molar refractivity as the two physical parameters depend on different properties of the medium, but it validates that our model can successfully predict the positive and negative deviation from ideality. This observation can be validated from previous thermodynamic studies also.[56−60] So, our proposed model of ThT quantum yield can successfully estimate the degree of solvent−solvent interaction and can predict non-ideality without any help from excess thermodynamic property measurements.

The key aspect of this study was to establish a relationship between φ_{ThT} values and the bulk viscosity of the solution. The viscosity coefficients for our experimental compositions of the methanol−glycerol mixture were obtained from a previous report and were directly used for calculations.[56] However, in the case of the ethanol−glycerol, *n*-butanol−glycerol, and *tert*-butanol−glycerol mixtures, viscosity coefficients were reported, but not specifically for the compositions studied here.[57−60] Hence, for these two cases, we applied the Grunberg−Nissan model to the available data and estimated the viscosity values according to our requirements.[61,62] A detailed analysis is provided in Supporting Information Scheme S2 and Figure S3. After conducting an extensive literature search, we discovered a lack of published data on the viscosity for the *n*-propanol−glycerol and *iso*-propanol−glycerol mixture. Consequently, this presented a unique opportunity for us to predict the bulk viscosity at various compositions of these two solvent mixtures based on the φ_{ThT} measurements.

Generally, the quantum yield of a molecular rotor has a power law relationship with viscosity commonly referred as the Förster−Hoffmann equation.[1,18,64] In this model, the power varies between 1/3 to 2/3. Loutfy and Arnold in their seminal work checked the validity of the model for molecular rotor dye over a large range of temperatures and in solvents comprising low to high viscosity.[64] They found the equation to be valid. If the measurement is performed at a constant temperature, then simply we can write

$$\varphi = B\eta^{\alpha} \tag{4}$$

Here, φ is the quantum yield of the molecular rotor, η is the viscosity coefficient, and B and α are the solvent- and probe-dependent constants. For ThT, we can write eq 4 taking logarithm in each side as

$$\log \varphi_{ThT} = \log\ B + \alpha \log \eta_{bulk} \tag{5}$$

In eq 5, η_{bulk} signifies the bulk viscosity of the solvent mixture. This equation establishes a linear relationship between log φ_{ThT} and log η_{bulk} with an intercept log B and slope α. Accordingly, we plotted log φ_{ThT} against log η_{bulk} for the four binary mixtures for which viscosity was reported, i.e., methanol−glycerol, ethanol−glycerol, *n*-butanol−glycerol, and *tert*-butanol−glycerol mixtures. These plots are listed in Figure 4. Here, it should be mentioned that the parameter log B is the same for pure solvents and different compositions of solvent mixture as all the solutions of ThT are homogeneous in nature. The first observation was that if we exclude the data point of pure glycerol in each of these four systems, the rest of the points follow a linear trend. The reason may be the excessively high viscosity of pure glycerol compared to the mixtures. While there may be other causes

https://doi.org/10.1021/acsomega.3c06428
ACS Omega 2023, 8, 36604−36613

related to excited-state dynamics, they are beyond the scope of this discussion here. Nonetheless, we fitted the data points excluding the point corresponding to pure glycerol, and parameters of the fit are reported in both the figure and Table 2. Perhaps, the most significant and intriguing finding is that the slope value (α) ranged only between 0.489 and 0.502. Considering the intrinsic error associated with the measurements, α values are extremely close to one another. It is to be noted that the experiment of *tert*-butanol−glycerol mixtures was performed at 30 °C, and still, we got a similar value for α. This fascinating finding suggests that the dependence of α on the solvent is minimal for the ThT and glycerol−monohydroxy alcohol mixture.

n-propanol and *iso*-propanol have a molecular weight and bulk viscosity value between the values of ethanol and *n*-butanol. So, from this analysis, we can safely assume that for the *n*-propanol−glycerol and *iso*-propanol−glycerol mixtures, α will have a similar value. We can use the estimated range of α to predict the bulk viscosity for different compositions of these two mixtures, which is not reported until now. The novelty of idea is that we can make this prediction without measuring the bulk viscosity. Since we do not have the knowledge about the intercept of the line, i.e., log *B*, we used the reported value of viscosity of pure *n*-propanol and *iso*-propanol in eq 5 to modify it as follows

$$\log \varphi_{\mathrm{ThT}}^{i} - \log \varphi_{\mathrm{ThT}}^{\mathrm{PrOH}} = \alpha(\log \eta_{\mathrm{bulk}}^{i} - \log \eta_{\mathrm{bulk}}^{\mathrm{PrOH}}) \quad (6)$$

Here, $\varphi_{\mathrm{ThT}}{}^{i}$ is the quantum yield of ThT in the *i*th composition of the mixture and $\varphi_{\mathrm{ThT}}{}^{\mathrm{PrOH}}$ is the same in pure *n*-propanol or *iso*-propanol. Similarly, $\eta_{\mathrm{bulk}}{}^{i}$ is the bulk viscosity of the *i*th composition of the mixture and $\eta_{\mathrm{bulk}}{}^{\mathrm{PrOH}}$ is the same for pure *n*-propanol or *iso*-propanol. So, we can calculate $\log \eta_{\mathrm{bulk}}{}^{i}$ as

$$\log \eta_{\mathrm{bulk}}^{i} = \frac{\log \varphi_{\mathrm{ThT}}^{i} - \log \varphi_{\mathrm{ThT}}^{\mathrm{PrOH}}}{\alpha} + \log \eta_{\mathrm{bulk}}^{\mathrm{PrOH}} \quad (7)$$

We used the value of α = 0.49 and 0.50 and calculated $\log \eta_{\mathrm{bulk}}{}^{i}$ for *n*-propanol−glycerol and *iso*-propanol−glycerol mixtures at25 °C. Employing 4, we have estimated the bulk viscosity ($\eta_{\mathrm{bulk}}{}^{i}$) for each of the α values for various compositions of *n*-propanol−glycerol and *iso*-propanol−glycerol mixtures, which is given in Table 3. In Figure 5, we have shown the variation of $\log \varphi_{\mathrm{ThT}}{}^{i}$ against $\log \eta_{\mathrm{bulk}}{}^{i}$ for α = 0.50 and variation of $\eta_{\mathrm{bulk}}{}^{i}$ with the mole fraction of glycerol for α = 0.50 in the two mixtures. The procedure discussed here can be employed to determine the bulk viscosity of an unknown composition of *n*-propanol−glycerol and *iso*-propanol−glycerol mixtures as well as can be used for other glycerol−monohydroxy alcohol mixtures.

4. CONCLUSIONS

The experiments and analysis performed in this work demonstrated the variation of quantum yield of ThT (φ_{ThT}) at different compositions of methanol−glycerol, ethanol−glycerol, *n*-propanol−glycerol, *iso*-propanol−glycerol, *n*-butanol−glycerol, and *tert*-butanol−glycerol solvent mixtures. With an increasing concentration of glycerol in the mixture, the φ_{ThT} values increased. We modeled the trend and estimated the deviation from ideality in each of mixtures. The extent of nonideality was found to vary as ethanol > *n*-Propanol > *n*-Butanol > *iso*-Propanol > methanol, whereas *tert*-butanol showed opposite deviation from ideality. This predictive model can be utilized to forecast the extent of nonideality resulting from solvent−solvent interactions for other binary mixtures too. A linear relationship between $\log \varphi_{\mathrm{ThT}}$ and $\log \eta_{\mathrm{bulk}}$ was established in four mixtures for which bulk viscosity is already known. The inference drawn from the analysis was used to develop our methodology to measure the bulk viscosity of glycerol−monohydroxy alcohol mixtures solely based on the quantum yield measurement. Applying it, we estimated and predicted the viscosity values for the previously unreported *n*-propanol−glycerol and *iso*-propanol−glycerol mixtures at several compositions. This analysis holds the potential to be

Table 3. Estimated Values of Viscosity Coefficient Using eq 7 for Different Compositions of Glycerol−*n*-Propanol and Glycerol−*iso*-Propanol Mixtures

X_1	X_2	viscosity (cP) for α = 0.490	viscosity (cP) for α = 0.500
		Glycerol (1) + *n*-Propanol (2)	
0.000	1.000	1.97	1.97
0.103	0.897	2.91	2.89
0.205	0.795	5.04	4.94
0.306	0.694	11.41	11.02
0.407	0.593	17.48	16.73
0.507	0.493	42.48	39.95
0.607	0.393	80.90	75.11
0.706	0.294	155.24	142.25
0.805	0.195	354.54	319.57
0.903	0.097	752.39	668.04
		Glycerol (1) + *iso*-Propanol (2)	
0.000	1.000	2.10	2.10
0.105	0.895	4.05	4.00
0.208	0.792	6.80	6.64
0.311	0.689	14.80	14.26
0.413	0.587	31.75	30.07
0.513	0.487	54.62	51.17
0.612	0.388	126.95	116.95
0.711	0.289	240.01	218.30
0.808	0.192	514.29	460.70
0.905	0.095	877.93	778.08

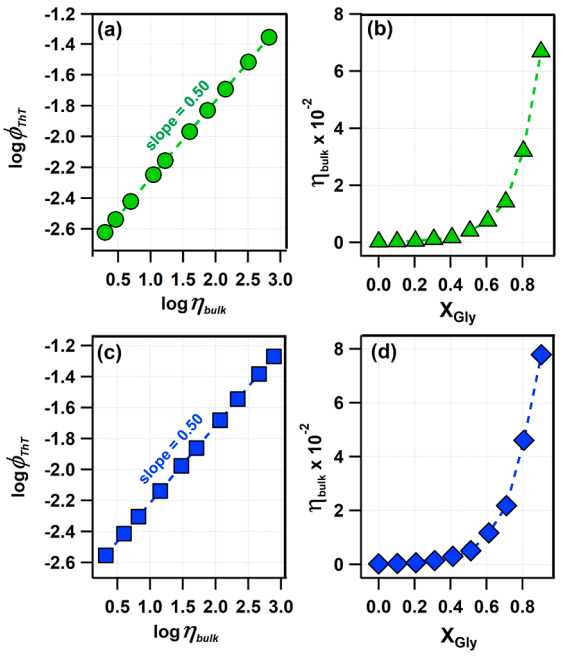

Figure 5. Plot of variation of $\log \varphi_{\mathrm{ThT}}$ against predicted $\log \eta_{\mathrm{bulk}}$ using eq 7 and estimated values of η_{bulk} against X_{Gly} (a), (b) *n*-propanol−glycerol (c) and (d) *iso*-propanol−glycerol.

https://doi.org/10.1021/acsomega.3c06428
ACS Omega 2023, 8, 36604−36613

extended to other solvents and biological systems, expanding its applicability and significance.

■ ASSOCIATED CONTENT

Supporting Information

The Supporting Information is available free of charge at https://pubs.acs.org/doi/10.1021/acsomega.3c06428.

Absorption spectra of thioflavin-T in different solvent mixtures; refractive index of binary mixtures of glycerol with methanol, ethanol, *n*-propanol, *iso*-propanol, *n*-butanol, and *tert*-butanol; and viscosity of ethanol−glycerol, *n*-butanol−glycerol, and *tert*-butanol−glycerol mixtures (PDF)

■ AUTHOR INFORMATION

Corresponding Authors

Puspal Mukherjee − *Department of Chemistry, School of Sciences, Netaji Subhas Open University, Kolkata, West Bengal 700064, India;* orcid.org/0000-0002-3693-672X; Email: puspalmukherjee.sosci@wbnsou.ac.in, puspalchem@gmail.com

Sintu Ganai − *Department of Chemistry, School of Sciences, Netaji Subhas Open University, Kolkata, West Bengal 700064, India;* orcid.org/0009-0004-2026-3307; Email: sintuganai.sosc@wbnsou.ac.in

Complete contact information is available at: https://pubs.acs.org/10.1021/acsomega.3c06428

Notes

The authors declare no competing financial interest.

■ ACKNOWLEDGMENTS

Puspal Mukherjee thanks Netaji Subhas Open University for funding vide project grant number Reg./1291 dated 22/11/2021, and Sintu Ganai thanks Netaji Subhas Open University for funding vide project grant number Reg./1289 dated 22/11/2021.

■ REFERENCES

(1) Groenning, M. Binding Mode of Thioflavin T and Other Molecular Probes in the Context of Amyloid Fibrils-Current Status. *J. Chem. Biol.* **2010**, *3* (1), 1−18.

(2) Freire, S.; De Araujo, M. H.; Al-Soufi, W.; Novo, M. Photophysical Study of Thioflavin T as Fluorescence Marker of Amyloid Fibrils. *Dyes Pigm.* **2014**, *110*, 97−105.

(3) Zou, M.; Yang, H.; Wang, H.; Wang, H.; Zhang, J.; Wei, B.; Zhang, H.; Xie, D. Detection of Type I Collagen Fibrils Formation and Dissociation by a Fluorescence Method Based on Thioflavin T. *Int. J. Biol. Macromol.* **2016**, *92*, 1175−1182.

(4) Xue, C.; Lin, T. Y.; Chang, D.; Guo, Z. Thioflavin T as an Amyloid Dye: Fibril Quantification, Optimal Concentration and Effect on Aggregation. *R. Soc. Open Sci.* **2017**, *4* (1), 160696.

(5) Tang, Z.; Liu, H.; Chen, M.; Ma, C. Label-Free One-Step Fluorescent Method for the Detection of Endonuclease Activity Based on Thioflavin T/G-Quadruplex. *Spectrochim. Acta, Part A* **2020**, *228*, 117823.

(6) Pramanik, S.; Nandy, A.; Chakraborty, S.; Pramanik, U.; Nandi, S.; Mukherjee, S. Preferential Binding of Thioflavin T to AT-Rich DNA: White Light Emission through Intramolecular Förster Resonance Energy Transfer. *J. Phys. Chem. Lett.* **2020**, *11* (7), 2436−2442.

(7) Chouchane, K.; Pignot-Paintrand, I.; Bruckert, F.; Weidenhaupt, M. Visible Light-Induced Insulin Aggregation on Surfaces via Photoexcitation of Bound Thioflavin T. *J. Photochem. Photobiol. B Biol.* **2018**, *181*, 89−97.

(8) Liu, Z.; Luo, X.; Li, Z.; Huang, Y.; Nie, Z.; Wang, H. H.; Yao, S. Enzyme-Activated G-Quadruplex Synthesis for in Situ Label-Free Detection and Bioimaging of Cell Apoptosis. *Anal. Chem.* **2017**, *89* (3), 1892−1899.

(9) Xu, S.; Li, Q.; Xiang, J.; Yang, Q.; Sun, H.; Guan, A.; Wang, L.; Liu, Y.; Yu, L.; Shi, Y.; Chen, H.; Tang, Y. Thioflavin T as an Efficient Fluorescence Sensor for Selective Recognition of RNA G-Quadruplexes. *Sci. Rep.* **2016**, *6* (1), 24793.

(10) Duxbury, D. F. The Photochemistry and Photophysics of Triphenylmethane Dyes in Solid and Liquid Media. *Chem. Rev.* **1993**, *93* (1), 381−433.

(11) Hawe, A.; Sutter, M.; Jiskoot, W. Extrinsic Fluorescent Dyes as Tools for Protein Characterization. *Pharm. Res.* **2008**, *25* (7), 1487−1499.

(12) Zhou, F.; Shao, J.; Yang, Y.; Zhao, J.; Guo, H.; Li, X.; Ji, S.; Zhang, Z. Molecular Rotors as Fluorescent Viscosity Sensors: Molecular Design, Polarity Sensitivity, Dipole Moments Changes, Screening Solvents, and Deactivation Channel of the Excited States. *Eur. J. Org Chem.* **2011**, *2011* (25), 4773−4787.

(13) Van Der Meer, M. J.; Zhang, H.; Glasbeek, M. Femtosecond Fluorescence Upconversion Studies of Barrierless Bond Twisting of Auramine in Solution. *J. Chem. Phys.* **2000**, *112* (6), 2878−2887.

(14) Maskevich, A. A.; Stsiapura, V. I.; Kuzmitsky, V. A.; Kuznetsova, I. M.; Povarova, O. I.; Uversky, V. N.; Turoverov, K. K. Spectral Properties of Thioflavin T in Solvents with Different Dielectric Properties and in a Fibril-Incorporated Form. *J. Proteome Res.* **2007**, *6* (4), 1392−1401.

(15) Stsiapura, V. I.; Maskevich, A. A.; Kuzmitsky, V. A.; Uversky, V. N.; Kuznetsova, I. M.; Turoverov, K. K. Thioflavin T as a Molecular Rotor: Fluorescent Properties of Thioflavin T in Solvents with Different Viscosity. *J. Phys. Chem. B* **2008**, *112* (49), 15893−15902.

(16) Ren, H.; Fingerhut, B. P.; Mukamel, S. Time Resolved Photoelectron Spectroscopy of Thioflavin T Photoisomerization: A Simulation Study. *J. Phys. Chem. A* **2013**, *117* (29), 6096−6104.

(17) Stsiapura, V. I.; Maskevich, A. A.; Kuzmitsky, V. A.; Turoverov, K. K.; Kuznetsova, I. M. Computational Study of Thioflavin T Torsional Relaxation in the Excited State. *J. Phys. Chem. A* **2007**, *111* (22), 4829−4835.

(18) Haidekker, M. A.; Theodorakis, E. A. Molecular Rotors - Fluorescent Biosensors for Viscosity and Flow. *Org. Biomol. Chem.* **2007**, *5* (11), 1669−1678.

(19) Lakowicz, J. R.. In *Principles of Fluorescence Spectroscopy*; Lakowicz, J. R., Ed.; Springer US: Boston, MA, 2006..

(20) Valeur, B.; Berberan-Santos, M. N. *Molecular Fluorescence*; Wiley, 2012..

(21) Erez, Y.; Liu, Y.-H.; Amdursky, N.; Huppert, D. Modeling the Nonradiative Decay Rate of Electronically Excited Thioflavin T. *J. Phys. Chem. A* **2011**, *115* (30), 8479−8487.

(22) Agmon, N.; Hopfield, J. J. Transient Kinetics of Chemical Reactions with Bounded Diffusion Perpendicular to the Reaction Coordinate: Intramolecular Processes with Slow Conformational Changes. *J. Chem. Phys.* **1983**, *78* (11), 6947−6959.

(23) Bagchi, B.; Fleming, G. R.; Oxtoby, D. W. Theory of Electronic Relaxation in Solution in the Absence of an Activation Barrier. *J. Chem. Phys.* **1983**, *78* (12), 7375−7385.

(24) Mukherjee, P.; Das, A.; Sen, P. Ultrafast Excited State Deactivation Channel of Thioflavin T Adsorbed on SDS Micelle: A Combined Femtosecond Fluorescence and Transient Absorption Study. *J. Photochem. Photobiol., A* **2017**, *348*, 287−294.

(25) Layek, S.; Bera, N.; Nandi, P. K.; Sarkar, N. Insights into the Strong Emission Enhancement of Molecular Rotor Thioflavin T in Aqueous Cellulose Nanocrystal Dispersion: White Light Generation in Protein and Micellar Media. *Langmuir* **2023**, *39* (23), 8083−8090.

(26) Singh, P. K.; Murudkar, S.; Mora, A. K.; Nath, S. Ultrafast Torsional Dynamics of Thioflavin-T in an Anionic Cyclodextrin Cavity. *J. Photochem. Photobiol., A* **2015**, *298*, 40−48.

(27) Mohanty, J.; Dutta Choudhury, S.; Upadhyaya, H. P.; Bhasikuttan, A. C.; Pal, H. Control of the Supramolecular Excimer Formation of Thioflavin T within a Cucurbit[8]Uril Host: A

Fluorescence on/off Mechanism. *Chem.—Eur. J.* **2009**, *15* (21), 5215−5219.
(28) Singh, P. K.; Kumbhakar, M.; Pal, H.; Nath, S. Viscosity Effect on the Ultrafast Bond Twisting Dynamics in an Amyloid Fibril Sensor: Thioflavin-T. *J. Phys. Chem. B* **2010**, *114* (17), 5920−5927.
(29) van der Meer, M. J.; Zhang, H.; Glasbeek, M. Femtosecond Fluorescence Upconversion Studies of Barrierless Bond Twisting of Auramine in Solution. *J. Chem. Phys.* **2000**, *112* (6), 2878−2887.
(30) Wei, H.; Tang, X.; Chen, Q.; Yue, T.; Dong, B. An Endoplasmic Reticulum-Targeting Fluorescent Probe for the Visualization of the Viscosity Fluctuations during Ferroptosis in Live Cells. *Anal. Chim. Acta* **2022**, *1232*, 340454.
(31) Priya, B.; Kumar, N.; Roopa. Photophysical Characterization of Coumarin and Rhodanine Derivatives as Viscosity Sensitive Fluorescence Turn-on Probes. *Dyes Pigm.* **2022**, *207*, 110707.
(32) Shi, W.-J.; Wei, Y.-F.; Yang, J.; Li, H.-Z.; Wan, Q.-H.; Wang, Y.; Leng, H.; Chen, K.; Yan, J. Novel Meso-Trifluoromethyl BODIPY-Based near-Infrared-Emitting Fluorescent Probes for Organelle-Specific Imaging of Cellular Viscosity. *Sens. Actuators, B* **2022**, *359*, 131594.
(33) Tantipanjaporn, A.; Kung, K. K.-Y.; Chan, W.-C.; Deng, J.-R.; Ko, B. C.-B.; Wong, M.-K. Quinolinium-Based Viscosity Probes for Lysosome Imaging and Tracing Lysosomal Viscosity Changes in Living Cells. *Sens. Actuators, B* **2022**, *367*, 132003.
(34) Singh, P. K.; Kumbhakar, M.; Pal, H.; Nath, S. Ultrafast Bond Twisting Dynamics in Amyloid Fibril Sensor. *J. Phys. Chem. B* **2010**, *114* (7), 2541−2546.
(35) Singh, P. K.; Kumbhakar, M.; Pal, H.; Nath, S. Ultrafast Torsional Dynamics of Protein Binding Dye Thioflavin-T in Nanoconfined Water Pool. *J. Phys. Chem. B* **2009**, *113* (25), 8532−8538.
(36) Singh, P. K.; Kumbhakar, M.; Pal, H.; Nath, S. Viscosity Effect on the Ultrafast Bond Twisting Dynamics in an Amyloid Fibril Sensor: Thioflavin-T. *J. Phys. Chem. B* **2010**, *114* (17), 5920−5927.
(37) Amdursky, N.; Gepshtein, R.; Erez, Y.; Huppert, D. Temperature Dependence of the Fluorescence Properties of Thioflavin-T in Propanol, a Glass-Forming Liquid. *J. Phys. Chem. A* **2011**, *115* (12), 2540−2548.
(38) Gautam, R. K.; Ahmed, S. A.; Seth, D. Photophysics of Thioflavin T in Deep Eutectic Solvents. *J. Lumin.* **2018**, *198*, 508−516.
(39) Singh, P. K.; Mora, A. K.; Nath, S. Free Volume Dependence of an Ionic Molecular Rotor in Fluoroalkylphosphate (FAP) Based Ionic Liquids. *Chem. Phys. Lett.* **2016**, *644*, 296−301.
(40) Stsiapura, V. I.; Maskevich, A. A.; Tikhomirov, S. A.; Buganov, O. V. Charge Transfer Process Determines Ultrafast Excited State Deactivation of Thioflavin T in Low-Viscosity Solvents. *J. Phys. Chem. A* **2010**, *114* (32), 8345−8350.
(41) Erez, Y.; Amdursky, N.; Gepshtein, R.; Huppert, D. Temperature and Viscosity Dependence of the Nonradiative Decay Rates of Auramine-O and Thioflavin-T in Glass-Forming Solvents. *J. Phys. Chem. A* **2012**, *116* (49), 12056−12064.
(42) Stsiapura, V. I.; Kurhuzenkau, S. A.; Kuzmitsky, V. A.; Bouganov, O. V.; Tikhomirov, S. A. Solvent Polarity Effect on Nonradiative Decay Rate of Thioflavin T. *J. Phys. Chem. A* **2016**, *120* (28), 5481−5496.
(43) Mukherjee, P.; Rafiq, S.; Sen, P. Dual Relaxation Channel in Thioflavin-T: An Ultrafast Spectroscopic Study. *J. Photochem. Photobiol., A* **2016**, *328*, 136−147.
(44) Ghosh, R.; Palit, D. K. Ultrafast Twisting Dynamics of Thioflavin-T: Spectroscopy of the Twisted Intramolecular Charge-Transfer State. *ChemPhysChem* **2014**, *15* (18), 4126−4131.
(45) Muhammad, A.; Mutalib, M. I. A.; Wilfred, C. D.; Murugesan, T.; Shafeeq, A. Viscosity, Refractive Index, Surface Tension, and Thermal Decomposition of Aqueous N-Methyldiethanolamine Solutions from (298.15 to 338.15) K. *J. Chem. Eng. Data* **2008**, *53* (9), 2226−2229.
(46) Ma, J.; Pang, Y.; Wang, M.; Xu, J.; Ma, H.; Nie, X. The Copolymerization Reactivity of Diols with 2,5-Furandicarboxylic Acid for Furan-Based Copolyester Materials. *J. Mater. Chem.* **2012**, *22* (8), 3457.
(47) Rodríguez, A.; Canosa, J.; Orge, B.; Iglesias, M.; Tojo, J. Mixing Properties of the System Methyl Acetate + Methanol + Ethanol at 298.15 K. *J. Chem. Eng. Data* **1996**, *41* (6), 1446−1449.
(48) Holmes, M. J.; Parker, N. G.; Povey, M. J. W. Temperature Dependence of Bulk Viscosity in Water Using Acoustic Spectroscopy. *J. Phys.: Conf. Ser.* **2011**, *269*, 012011.
(49) Dukhin, A. S.; Goetz, P. J. Bulk Viscosity and Compressibility Measurement Using Acoustic Spectroscopy. *J. Chem. Phys.* **2009**, *130* (12), 124519.
(50) Rafiq, S.; Yadav, R.; Sen, P. Microviscosity inside a Nanocavity: A Femtosecond Fluorescence up-Conversion Study of Malachite Green. *J. Phys. Chem. B* **2010**, *114* (44), 13988−13994.
(51) Raut, S. L.; Kimball, J. D.; Fudala, R.; Bora, I.; Chib, R.; Jaafari, H.; Castillo, M. K.; Smith, N. W.; Gryczynski, I.; Dzyuba, S. V.; Gryczynski, Z. A Triazine-Based BODIPY Trimer as a Molecular Viscometer. *Phys. Chem. Chem. Phys.* **2016**, *18* (6), 4535−4540.
(52) Cano-Gómez, J. J.; Iglesias-Silva, G. A.; Ramos-Estrada, M.; Hall, K. R. Densities and Viscosities for Binary Liquid Mixtures of Ethanol + 1-Propanol, 1-Butanol, and 1-Pentanol from (293.15 to 328.15) K at 0.1 MPa. *J. Chem. Eng. Data* **2012**, *57* (9), 2560−2567.
(53) Canosa, J.; Rodríguez, A.; Tojo, J. Dynamic Viscosities of (Methyl Acetate or Methanol) with (Ethanol, 1-Propanol, 2-Propanol, 1-Butanol, and 2-Butanol) at 298.15 K. *J. Chem. Eng. Data* **1998**, *43* (3), 417−421.
(54) Kuimova, M. K.; Yahioglu, G.; Levitt, J. A.; Suhling, K. Molecular Rotor Measures Viscosity of Live Cells via Fluorescence Lifetime Imaging. *J. Am. Chem. Soc.* **2008**, *130* (21), 6672−6673.
(55) *CRC Handbook of Chemistry and Physics*; Haynes, W. M., Ed.CRC Press, 2014..
(56) Levitt, J. A.; Chung, P. H.; Kuimova, M. K.; Yahioglu, G.; Wang, Y.; Qu, J.; Suhling, K. Fluorescence Anisotropy of Molecular Rotors. *ChemPhysChem* **2011**, *12* (3), 662−672.
(57) Koohyar, F.; Nasiri, J.; Kiani, F. Refractometric Study on Binary, Ternary, and Quaternary Solutions Made by Water, Methanol, Ethanol, Glycerol, D-Glucose Monohydrate (DGMH), Sucrose, and Sodium Chloride at T = 293.15 K and Atmospheric Pressure. *J. Mex. Chem. Soc.* **2019**, *62* (4), 160.
(58) Valat, P.; Wintgens, V.; Kossanyi, J.; Biczok, L.; Demeter, A.; Berces, T. Influence of Geometry on the Emitting Properties of 2,3-Naphthalimides. *J. Am. Chem. Soc.* **1992**, *114* (3), 946−953.
(59) Valente, M. P.; De Paula, I. B. Sensor Based on Piezo Buzzers for Simultaneous Measurement of Fluid Viscosity and Density. *Measurement* **2020**, *152*, 107308.
(60) Chabouni, Y.; Amireche, F. Some Physicochemical Properties of Binary Mixtures of Glycerol with Butanol Isomers in the Temperature Range 293.15−318.15 K and Ambient Pressure. *J. Chem. Eng. Data* **2020**, *65* (4), 1679−1694.
(61) Grunberg, L.; Nissan, A. H. Mixture Law for Viscosity. *Nature* **1949**, *164* (4175), 799−800.
(62) Viswanath, D. S.; Ghosh, T. K.; Prasad, D. H. L.; Dutt, N. V. K.; Rani, K. Y. Viscosities of Solutions and Mixtures. In *Viscosity of Liquids*; Springer Netherlands: Dordrecht, 2007; pp 407−442..
(63) Gupta, S.; Rafiq, S.; Sen, P. Dynamics of Solvent Response in Methanol-Chloroform Binary Solvent Mixture: A Case of Synergistic Solvation. *J. Phys. Chem. B* **2015**, *119* (7), 3135−3141.
(64) Loutfy, R. O.; Arnold, B. A. Effect of Viscosity and Temperature on Torsional Relaxation of Molecular Rotors. *J. Phys. Chem.* **1982**, *86* (21), 4205−4211.

https://doi.org/10.1021/acsomega.3c06428
ACS Omega 2023, 8, 36604−36613